

Hadamard Wirtinger Flow for Sparse Phase Retrieval

Fan Wu, Patrick Rebeschini
Department of Statistics, University of Oxford

June 2, 2020

Abstract

We consider the problem of reconstructing an n -dimensional k -sparse signal from a set of magnitude-only measurements. Formulating the problem as an unregularized empirical risk minimization task, we study the sample complexity performance of gradient descent with Hadamard parametrization, which we call Hadamard Wirtinger flow (HWF). Provided knowledge of the signal sparsity k , we prove that a single step of HWF is able to recover the support from $\mathcal{O}(k(x_{max}^*)^{-2} \log n)$ samples, where x_{max}^* is the largest component of the signal in magnitude. This support recovery procedure can be used to initialize existing reconstruction methods and yields algorithms with total runtime proportional to the cost of reading the data and improved sample complexity, which is linear in k when the signal contains at least one large component. We numerically investigate the performance of HWF at convergence and show that, while not requiring any explicit form of regularization nor knowledge of k , HWF adapts to the signal sparsity and reconstructs sparse signals with fewer measurements than existing state-of-the-art methods.

1 Introduction

Phase retrieval, the problem of reconstructing a signal from the (squared) magnitude of its Fourier (or any linear) transform, arises in many fields of science and engineering. Such a task is naturally involved in applications such as crystallography (Millane, 1990) and diffraction imaging (Bunk et al., 2007), where optical sensors are able to measure the intensity, but not the phase of a light wave. Due to the loss of phase information, the one-dimensional Fourier phase retrieval problem is ill-posed in general. Common approaches to overcome this ill-posedness include using prior information such as non-negativity, sparsity and the signal’s magnitude (Fienup, 1982; Jaganathan et al., 2016), or introducing redundancy into the measurements by oversampling random Gaussian measurements or coded diffraction patterns (Candès et al., 2015; Chen and Candès, 2015).

In many applications, the underlying signal is naturally sparse (Jaganathan et al., 2016). A wide range of algorithms has been devised for phase retrieval with a sparse signal, including alternating minimization (SparseAltMinPhase) (Netrapalli et al., 2015), non-convex optimization based approaches such as thresholded Wirtinger flow (TWF) (Cai et al., 2016), sparse truncated amplitude flow (SPARTA) (Wang et al., 2018), compressive reweighted amplitude flow (CRAF) (Zhang et al., 2018) and sparse Wirtinger flow (SWF) (Yuan et al., 2019), and convex relaxation methods such as compressive phase retrieval via lifting (CPRL) (Ohlsson et al., 2012) and SparsePhaseMax (Hand and Voroninski, 2016). Other approaches to sparse phase retrieval include the greedy algorithm GESPAR (Schechtman et al., 2014), an algorithm based on generalized

approximate message passing (PR-GAMP) (Schniter and Rangan, 2015) and majorization minimization algorithms (Qiu and Palomar, 2017).

A limitation of these algorithms is their sample complexity: the best known theoretical results require $\mathcal{O}(k^2 \log n)$ Gaussian measurements to guarantee successful reconstruction of a generic k -sparse signal $\mathbf{x}^* \in \mathbb{R}^n$. On the other hand, it has been shown that reconstruction is possible from $\mathcal{O}(k \log n)$ phaseless measurements (Eldar and Mendelson, 2014); however, there is no known algorithm which achieves this in polynomial time. In fact, $\mathcal{O}(k^2 \log n)$ quadratic measurements are necessary for a certain class of convex relaxations, on which algorithms such as CPRL are based (Li and Voroninski, 2013). Other existing algorithms such as SPARTA and SparseAltMinPhase require a sample complexity of $\mathcal{O}(k^2 \log n)$ for the initial estimation of the support of the signal. With the knowledge of the support, these (and plenty other) algorithms require only $\mathcal{O}(k \log n)$ samples for the subsequent reconstruction of the signal. Hence, we identify the support recovery step as the bottleneck of the sample complexity of non-convex optimization based approaches to the sparse phase retrieval problem.

Additional structural assumptions have been considered to improve the sample complexity. It has been shown that a k -sparse signal \mathbf{x}^* can be reconstructed from $\mathcal{O}(k \log n)$ measurements if one is allowed to freely design the measurement vectors (Jaganathan et al., 2013), or if the signal \mathbf{x}^* is assumed to be block-sparse and the number of blocks containing non-zero entries is $\mathcal{O}(1)$ (Jagatap and Hedge, 2017; Zhang et al., 2018). However, exact knowledge of the additional structure as well as an algorithm designed to take advantage of it is necessary in both cases. Linear sample complexity has also been achieved using the assumption that the signal coefficients decay with power-law (Jagatap and Hedge, 2019).

Another downside of the above algorithms is the fact that sparsity is enforced or promoted *explicitly*. For instance, CPRL and SparsePhaseMax augment the objective function with an ℓ_1 penalty term, which is known to promote sparsity. SWF and SPARTA include a thresholding step in their gradient updates, which projects the iterates onto the set of k -sparse vectors, and SparseAltMinPhase and GESPAR directly constrain the search to a k -dimensional subspace of \mathbb{R}^n , which needs to be carefully chosen and updated. This means that, in the case of CPRL and SparsePhaseMax, additional regularization parameters have to be tuned, while the thresholding step of SWF and SPARTA requires knowledge of the signal sparsity k .

1.1 Our Contributions

In this work, we analyze gradient descent with Hadamard parametrization applied to the unregularized empirical risk for sparse phase retrieval and propose methods for support recovery and parameter estimation. The main contributions of this paper are stated below.

First, we propose a two-stage procedure for sparse phase retrieval, which we call *Hadamard Wirtinger flow* (HWF) (following the terminology used for Wirtinger flow (Candès et al., 2015), which considers gradient descent applied to the unregularized empirical risk under the natural parametrization to solve phase retrieval without the assumption on sparsity). In stage one, we estimate a *single* coordinate on the support to construct a simple initial estimate, without using a sophisticated initialization scheme typically required such as the spectral initialization used in WF and SWF or the orthogonality-promoting initialization used in SPARTA. For stage two, we consider the Hadamard parametrization, which has previously been applied to problems on sparse recovery (Hoff, 2017; Vaškevičius et al., 2019; Zhao et al., 2019) and matrix factorization (Gunasekar et al., 2017; Li et al., 2018; Arora et al., 2019), and apply gradient descent to the unregularized empirical risk under this parametrization.

Second, we prove that our proposed algorithm can be used to recover the support $S = \{i : x_i^* \neq 0\}$ with high probability by choosing the k largest components of the estimate obtained after one step of HWF, provided that $m \geq \mathcal{O}(k(x_{max}^*)^{-2} \log n)$ and $x_{min}^* = \mathcal{O}(1/\sqrt{k})$, where we write $x_{max}^* := \max_i |x_i^*|/\|\mathbf{x}^*\|_2$ and $x_{min}^* := \min_{i:x_i^* \neq 0} |x_i^*|/\|\mathbf{x}^*\|_2$. With the knowledge of the support S , plenty of algorithms provably recover the signal \mathbf{x}^* under linear sample complexity $\mathcal{O}(k \log n)$, e.g. (Candès and Li, 2012; Chen and Candès, 2015; Wang et al., 2018). Thus, provided knowledge of the sparsity level k , one step of HWF can be used as a support recovery tool and, combined with any of the aforementioned algorithms, it results in a procedure which provably recovers a k -sparse signal $\mathbf{x}^* \in \mathbb{R}^n$ from $\mathcal{O}(k(x_{max}^*)^{-2} \log n)$ phaseless measurements.

If $x_{max}^* = \mathcal{O}(1)$, then the sample complexity of this procedure reduces to $\mathcal{O}(k \log n)$. Unlike previous results which leverage additional structural assumptions to achieve linear sample complexity, our procedure does not require knowledge of the value of x_{max}^* , nor it needs to be modified in any way to accommodate for this additional structure; in fact, we run the exact same algorithm regardless of what value x_{max}^* takes.

Third, we present numerical experiments showing the low sample complexity of HWF. As a simple algorithm not requiring thresholding steps nor added regularization terms to promote sparsity, HWF is seen to *adapt* to the sparsity level of the underlying signal and to reconstruct signals from a similar number of Gaussian measurements as PR-GAMP, which has been empirically shown to achieve linear sample complexity in some regimes with Gaussian signals (Schniter and Rangan, 2015). In particular, the numerical experiments suggest that the sample complexity required by HWF is lower than that of other gradient based methods such as SPARTA and SWF. Further, if the signal satisfies $x_{max}^* = \mathcal{O}(1)$, the reconstruction performance of HWF is seen to be greatly improved, without any modifications to the algorithm being made.

2 Sparse Phase Retrieval

We denote vectors and matrices with boldface letters and real numbers with normal font, and, where appropriate, use uppercase letters for random and lowercase letters for deterministic quantities. For vectors $\mathbf{u}, \mathbf{v} \in \mathbb{R}^n$ we write \odot for the Hadamard product, $(\mathbf{u} \odot \mathbf{v})_i = u_i v_i$, and, for notational simplicity, $\mathbf{u}^2 = \mathbf{u} \odot \mathbf{u}$ for taking squares entry-wise. We use the common notation $[n] := \{1, \dots, n\}$. Since it is impossible to distinguish \mathbf{x}^* from $-\mathbf{x}^*$ using magnitude-only observations, we will often write \mathbf{x}^* for the solution set $\{\pm \mathbf{x}^*\}$ and consider, for any $\mathbf{x} \in \mathbb{R}^n$, the distance $\text{dist}(\mathbf{x}, \mathbf{x}^*) := \min\{\|\mathbf{x} - \mathbf{x}^*\|_2, \|\mathbf{x} + \mathbf{x}^*\|_2\}$. Further, we will always assume $\|\mathbf{x}^*\|_2 = 1$. Note that this assumption is only for notational simplicity and not needed for our results.

The goal in phase retrieval is to reconstruct an unknown signal vector $\mathbf{x}^* \in \mathbb{R}^n$ from a set of quadratic measurements

$$Y_j = (\mathbf{A}_j^T \mathbf{x}^*)^2, \quad j = 1, \dots, m, \quad (1)$$

where $\mathbf{A}_j \sim \mathcal{N}(0, \mathbf{I}_n)$ i.i.d. are observed. For the sake of clarity, we focus on the real-valued model. Our proposed algorithm also works in the complex-valued Gaussian model, where $\mathbf{x}^* \in \mathbb{C}^n$ and $\mathbf{A}_j \sim \mathcal{N}(0, \frac{1}{2}\mathbf{I}_n) + i\mathcal{N}(0, \frac{1}{2}\mathbf{I}_n)$.

Many methods have been devised to solve this problem. A popular class of algorithms performs alternating projections onto different constraint sets; these include the seminal error reduction algorithm proposed by Gerchberg and Saxton (1972) and alternating minimization (AltMinPhase) (Netrapalli et al., 2015). Another more recent approach is based on non-convex optimization: Wirtinger flow (WF) (Candès et al., 2015) and its variants (Chen and Candès, 2015; Zhang et al., 2017), truncated amplitude flow (TAF) (Wang et al., 2017) and the trust region method

of (Sun et al., 2018) all minimize the empirical risk (which is non-convex due to the missing phase) based on different loss functions. The convex alternatives typically use matrix-lifting as in PhaseLift (Candès and Li, 2012; Candès et al., 2013) and PhaseCut (Waldspurger et al., 2015), which allows phase retrieval to be formulated as a semidefinite programming problem, or consider a non-lifting convex relaxation and solve the dual problem as in PhaseMax (Goldstein and Studer, 2018).

Our approach for estimating the signal \mathbf{x}^* follows the established approach of empirical risk minimization. Writing $\mathbf{z} = (y, \mathbf{a}) \in \mathbb{R} \times \mathbb{R}^n$ for an observation, we consider the loss function $\ell(\mathbf{x}, \mathbf{z}) = \frac{1}{4}((\mathbf{a}^T \mathbf{x})^2 - y)^2$ and, given samples $\mathbf{Z}_1, \dots, \mathbf{Z}_m$, the empirical risk

$$F(\mathbf{x}) = \frac{1}{m} \sum_{j=1}^m \ell(\mathbf{x}, \mathbf{Z}_j) = \frac{1}{4m} \sum_{j=1}^m \left((\mathbf{A}_j^T \mathbf{x})^2 - Y_j \right)^2. \quad (2)$$

It is worth mentioning that in previous applications the amplitude-based loss function $\ell(\mathbf{x}, \mathbf{z}) = \frac{1}{2}(|\mathbf{a}^T \mathbf{x}| - \sqrt{y})^2$ has been numerically shown to be more effective in terms of sample complexity than the loss function based on squared magnitudes (Wang et al., 2017; Zhang et al., 2017; Wang et al., 2018). However, with our parametrization, we found the squared magnitude-based loss function to be more effective.

Without any restrictions on the signal $\mathbf{x}^* \in \mathbb{R}^n$, $m \geq 2n - 1$ Gaussian measurements suffice for \mathbf{x}^* to be the unique (up to global sign) minimizer of $F(\mathbf{x})$ with high probability (Balan et al., 2006). If we assume \mathbf{x}^* to be k -sparse, then it has been shown in (Li and Voroninski, 2013) that

$$\{\pm \mathbf{x}^*\} = \underset{\mathbf{x}: \|\mathbf{x}\|_0 \leq k}{\operatorname{argmin}} F(\mathbf{x}) \quad (3)$$

holds with high probability if we have $m \geq 4k - 1$ Gaussian measurements.

Solving (3) involves two main difficulties: (i) the objective function F is non-convex with potentially many local minima and saddle points, and (ii) due to the constraint $\|\mathbf{x}\|_0 \leq k$ the problem is of combinatorial nature and NP-hard in general.

Regarding the first difficulty, the non-convexity is typically addressed by using a spectral or orthogonality-promoting initialization, which produces an initial estimate close to \mathbf{x}^* and in a region where the the objective function is locally strongly convex, leading to linear convergence towards \mathbf{x}^* (Candès et al., 2015; Chen and Candès, 2015; Wang et al., 2017; Zhang et al., 2017). Recently, it has been shown that such an initialization is not always necessary in the phase retrieval problem and that a random initialization can be used instead (Sun et al., 2018; Chen et al., 2019).

Addressing the second difficulty, an approach replacing the constraint $\|\mathbf{x}\|_0 \leq k$ in (3) by adding a penalty term $\lambda \|\mathbf{x}\|_1$ was proposed in (Yang et al., 2013). However, this procedure requires tuning of the regularization parameter λ to reach a desired sparsity level, and it is tailored for Fourier measurements only (in particular, it uses the fact that the DFT matrix is unitary). Recently, methods enforcing the constraint $\|\mathbf{x}\|_0 \leq k$ via a hard-thresholding step have received a lot of attention. These include SPARTA (Wang et al., 2018), CRAF (Zhang et al., 2018) and SWF (Yuan et al., 2019). However, the implementation of such a thresholding step requires knowledge of k (or a suitable upper bound).

Our proposed method does not have to deal with these difficulties. We also approach the problem by minimizing the objective $F(\mathbf{x})$. However, unlike existing algorithms, we do not need to add any penalty term to the objective or to introduce a thresholding step to enforce the constraint $\|\mathbf{x}\|_0 \leq k$. Our simulations show that the iterates of gradient descent with Hadamard

parametrization remain (approximately) in the low-dimensional space of sparse vectors. Hence, we neither need to tune any regularization parameters, nor do we need knowledge of the underlying signal sparsity. Further, HWF does not need the sophisticated initialization scheme commonly used in non-convex optimization based approaches to (sparse) phase retrieval.

3 Hadamard Wirtinger Flow

Consider the parametrization $\mathbf{x} = \mathbf{u} \odot \mathbf{u} - \mathbf{v} \odot \mathbf{v}$. Such a parametrization has previously been applied to problems such as sparse recovery (Hoff, 2017; Vaškevičius et al., 2019; Zhao et al., 2019) and matrix factorization (Gunasekar et al., 2017; Li et al., 2018; Arora et al., 2019). Exploiting the restricted isometry property (RIP) assumed for these problems, the Hadamard parametrization has been shown to confine the gradient iterates to the low-dimensional spaces of sparse vectors and low-rank matrices, respectively.

Overloading the notation, we write the objective function as

$$F(\mathbf{u}, \mathbf{v}) = \frac{1}{4m} \sum_{j=1}^m ((\mathbf{A}_j^T(\mathbf{u}^2 - \mathbf{v}^2))^2 - Y_j)^2,$$

with gradients

$$\nabla_{\mathbf{u}} F(\mathbf{u}, \mathbf{v}) = \frac{2}{m} \sum_{j=1}^m ((\mathbf{A}_j^T(\mathbf{u}^2 - \mathbf{v}^2))^2 - (\mathbf{A}_j^T \mathbf{x}^*)^2) \cdot (\mathbf{A}_j^T(\mathbf{u}^2 - \mathbf{v}^2)) \mathbf{A}_j \odot \mathbf{u} = 2\nabla F(\mathbf{x}) \odot \mathbf{u},$$

and, similarly, $\nabla_{\mathbf{v}} F(\mathbf{u}, \mathbf{v}) = -2\nabla F(\mathbf{x}) \odot \mathbf{v}$. We consider gradient descent in this parametrization, where the additive gradient updates correspond to multiplicative updates on \mathbf{u} and \mathbf{v} . Denote by $\mathbf{1}_n \in \mathbb{R}^n$ the vector of all ones.

Algorithm 1: Gradient Descent, Hadamard parametrization

Input: observations $\{Y_j\}_{j=1}^m$, measurement vectors $\{\mathbf{A}_j\}_{j=1}^m$, step size η , iterations T , initialization $\mathbf{U}^0, \mathbf{V}^0$

Set $\mathbf{X}^0 = \mathbf{U}^0 \odot \mathbf{U}^0 - \mathbf{V}^0 \odot \mathbf{V}^0$

for $t = 1$ **to** T **do**

$$\mathbf{U}^t = \mathbf{U}^{t-1} \odot (\mathbf{1}_n - 2\eta \nabla F(\mathbf{X}^{t-1}))$$

$$\mathbf{V}^t = \mathbf{V}^{t-1} \odot (\mathbf{1}_n + 2\eta \nabla F(\mathbf{X}^{t-1}))$$

$$\mathbf{X}^t = \mathbf{U}^t \odot \mathbf{U}^t - \mathbf{V}^t \odot \mathbf{V}^t$$

end for

Return: \mathbf{X}^T

The reason why the Hadamard parametrization promotes sparsity is that this parametrization turns the additive updates of gradient descent into multiplicative updates. If we choose a small initialization, then, in the aforementioned problems with RIP assumptions, the multiplicative updates were shown to lead to off-support variables staying negligibly small while on-support variables are being fitted. The variables grow exponentially, but at different (time-varying) rates, with off-support variables growing at a smaller rate than on-support variables. With additive updates, off-support variables would not stay sufficiently small and the algorithm would typically converge towards non-sparse local minima.

The problem of sparse phase retrieval that we consider is known to satisfy the RIP property, cf. (Voroninski and Xu, 2016) for instance, and a similar explanation on why on-support variables and off-support variables can be made to grow at different speeds also holds in our setting. We now provide the main intuition behind the convergence properties of HWF by considering the evolution of the algorithm at the population level, i.e. in the case when $m = \infty$. While a rigorous convergence investigation of HWF is outside the scope of the current submission, the analysis that we now provide is instrumental to construct a good initialization for Algorithm 1.

Consider the simplified setting where \mathbf{x}^* is non-negative, i.e. $x_i^* \geq 0$ for all i . We can set $\mathbf{v} = \mathbf{0}$ in the parametrization, so that $\mathbf{x} = \mathbf{u}^2$. Further, assume that we have access to the population risk $f(\mathbf{x}) := \mathbb{E}[\ell(\mathbf{x}, \mathbf{Z})]$ (in other words, $m = \infty$), where $\mathbf{Z} = (Y, \mathbf{A})$ is defined as in (1). Its gradient can be computed as

$$\nabla f(\mathbf{x}) = (3\|\mathbf{x}\|_2^2 - 1)\mathbf{x} - 2(\mathbf{x}^T \mathbf{x}^*)\mathbf{x}^*. \quad (4)$$

Under these two assumptions, first consider the initialization $\mathbf{x}^0 = \alpha^2 \mathbf{1}_n$ for some small constant $\alpha > 0$. We can directly track the evolution of the estimates \mathbf{x}^t (note that we use lowercase letters, since with $m = \infty$ the sequence is not random anymore) generated by Algorithm 1 via

$$x_i^{t+1} = x_i^t \left(1 - 2\eta \left[(3\|\mathbf{x}^t\|_2^2 - 1)x_i^t - 2(\mathbf{x}^t)^T \mathbf{x}^* x_i^* \right] \right)^2.$$

This suggests that the evolution of \mathbf{x}^t can be divided into two phases: if $\|\mathbf{x}^t\|_2^2 < \frac{1}{3}$, all coordinates grow ($x_i^{t+1} > x_i^t$), while coordinates $i \in S$ on the support do so at a faster rate. If $\|\mathbf{x}^t\|_2^2 > \frac{1}{3}$, coordinates $i \notin S$ decrease ($x_i^{t+1} < x_i^t$), while coordinates on the support increase if the product of the signal component x_i^* and the inner product $(\mathbf{x}^t)^T \mathbf{x}^*$ is larger than the term $(3\|\mathbf{x}^t\|_2^2 - 1)x_i^t$.

If we choose $\alpha > 0$ small enough, we expect x_j^t to still be small (e.g. $< 1/n$) for $j \notin S$ when $\|\mathbf{x}^t\|_2^2 \geq \frac{1}{3}$ first occurs, as x_i^t grows at a faster rate than x_j^t for $i \in S$. Since x_j^t decreases for $j \notin S$ when $\|\mathbf{x}^t\|_2^2 \geq \frac{1}{3}$, we expect x_j^t to stay small throughout the algorithm for $j \notin S$.

The smaller the step size η is, the more iterations are needed for the algorithm to converge. On the other hand, η cannot be too large; to illustrate this, consider $n = 1$. The (scalar) gradient update becomes $x^{t+1} = x^t(1 - 6\eta[(x^t)^3 - x^t])$, and x^t diverges if η is too large. We found a constant step size $\eta = 0.1$ to work well in our simulations.

This recursion has three types of fixed points: $\mathbf{x}^{(1)} = \mathbf{0}$, any $\mathbf{x}^{(2)}$ satisfying $\|\mathbf{x}^{(2)}\|_2^2 = \frac{1}{3}$ and $(\mathbf{x}^{(2)})^T \mathbf{x}^* = 0$, and $\mathbf{x}^{(3)} = \pm \mathbf{x}^*$. The first fixed point $\mathbf{x}^{(1)}$ is repelling, as all coordinates grow if $\|\mathbf{x}^t\|_2^2 < \frac{1}{3}$. Similarly, the second fixed point $\mathbf{x}^{(2)}$ is repelling as x_i^t grows at a faster rate than x_j^t for $i \in S, j \notin S$. This leaves only $\mathbf{x}^{(3)}$, which is an attracting fixed point of the recursion. Thus, we expect Algorithm 1 to converge to \mathbf{x}^* if m is sufficiently large.

Guided by this intuition, we aim to construct an initialization \mathbf{X}^0 with $(\mathbf{X}^0)^T \mathbf{x}^*$ large (more precisely, we will have $|(\mathbf{X}^0)^T \mathbf{x}^*| \geq \frac{1}{4}x_{max}^*$), while at the same time $\|\mathbf{X}^0\|_2^2$ should not be too large (e.g. fixed to $\|\mathbf{X}^0\|_2^2 = \frac{1}{3}$; note that, in fact, any other constant would also work). In order to obtain such an initialization, it suffices to find a coordinate i with $|x_i^*| \geq \frac{1}{2}x_{max}^*$. Then, we can set $X_i^0 = 1/\sqrt{3}$ and $X_j^0 = 0$ for all $j \neq i$.

Define the random variables $R_i = \frac{1}{m} \sum_{j=1}^m Y_j A_{ji}^2$. These quantities were also used in (Wang et al., 2018) for support recovery, as one can compute $\mathbb{E}[R_i] = \|\mathbf{x}^*\|_2^2 + 2x_i^2$ using the assumption $\mathbf{A}_j \sim \mathcal{N}(0, \mathbf{I}_n)$ i.i.d.. Hence, if the number of measurements m is large, the random variables $\{R_i\}$ will concentrate around their means, separating them for $i \in S$ and $i \notin S$. This intuition suggests the procedure summarized in Algorithm 2.

Algorithm 2: Initialization for Algorithm 1

Input: observations $\{Y_j\}_{j=1}^m$, measurement vectors $\{\mathbf{A}_j\}_{j=1}^m$, initialization size α

Set $i_{max} = \operatorname{argmax}_{i \in [n]} \frac{1}{m} \sum_{j=1}^m Y_j A_{ji}^2$

Set $\mathbf{U}^0 = \mathbf{V}^0 = \alpha \mathbf{1}_n$, $U_{i_{max}}^0 = \left(\sqrt{\frac{1}{3}} + \alpha^2\right)^{\frac{1}{2}}$

Return: $\mathbf{U}^0, \mathbf{V}^0$

We will show in the next section that the largest instance in the collection $\{R_i\}$ corresponds to a coordinate i with $|x_i^*| \geq \frac{1}{2}x_{max}^*$ with high probability if m is sufficiently large, in which case Algorithm 2 leads to an initialization \mathbf{X}^0 satisfying $|(\mathbf{X}^0)^T \mathbf{x}^*| \geq \frac{1}{4}x_{max}^*$ and $\|\mathbf{X}^0\|_2^2 = \frac{1}{3}$. While we use the same quantities $\{R_i\}$ as in (Wang et al., 2018), we only need to find a single coordinate i satisfying $|x_i^*| \geq \frac{1}{2}x_{max}^*$ rather than the full support, which allows us to improve the sample complexity compared to (Wang et al., 2018).

Finally, we can increase the probability of finding a large coordinate i and therefore a desirable initialization \mathbf{X}^0 if we allow multiple restarts and consider not only the largest, but also a few more instances in $\{R_i\}$. Specifically, if we allow B restarts, we consider different initialization as in Algorithm 2 using each of the B largest instances in $\{R_i\}$.

As pointed out in Section 2, \mathbf{x}^* is the sparsest minimizer of the objective F . Given the results from multiple runs of Algorithm 1, we can therefore choose the (approximately) sparsest solution, by which we mean the solution where the fewest coordinates make up most (e.g. 95%) of the norm $\|\mathbf{X}^T\|_2$. This is summarized in Algorithm 3.

Algorithm 3: Hadamard Wirtinger Flow, multiple restarts

Input: observations $\{Y_j\}_{j=1}^m$, measurement vectors $\{\mathbf{A}_j\}_{j=1}^m$, step size η , iterations T , initialization size α , number of restarts B , sparsity tolerance κ

Set i_1, \dots, i_B to the B largest instances in $\{\frac{1}{m} \sum_{j=1}^m Y_j A_{ji}^2\}$

for $b = 1$ **to** B **do**

Set $\mathbf{U}^0 = \mathbf{V}^0 = \alpha \mathbf{1}_n$, $U_{i_b}^0 = \left(\sqrt{\frac{1}{3}} + \alpha^2\right)^{\frac{1}{2}}$

Run Algorithm 1 with initialization $(\mathbf{U}^0, \mathbf{V}^0)$ for $\mathbf{X}^{T,b}$

end for

Set b_{min} to be the index which minimizes

$$\min_{C \subset [n]} \left\{ |C| : \sum_{i \in C} (\mathbf{X}_i^{T,b})^2 \geq (1 - \kappa) \sum_{i=1}^n (\mathbf{X}_i^{T,b})^2 \right\}$$

Return: $\mathbf{X}^{T,b_{min}}$

4 Support Recovery

In this section we show that, assuming $x_{min}^* = \mathcal{O}(1/\sqrt{k})$, one step of Algorithm 3 can be used to recover the support S from $\mathcal{O}(k(x_{max}^*)^{-2} \log n)$ Gaussian measurements. As pointed out in Section 2, the sample complexity bottleneck of reconstruction algorithms such as SPARTA and SparseAltMinPhase lies in the initial support recovery. In particular, both algorithms require $\mathcal{O}(k^2 \log n)$ measurements to guarantee successful support recovery; with the knowledge of the

support S , these and plenty other algorithms such as WF, TAF and PhaseLift only require a sample complexity of $\mathcal{O}(k \log n)$ to guarantee successful reconstruction of a k -sparse signal \mathbf{x}^* .

The main difference from previous work is that we only need to find a single coordinate i with $|x_i^*| \geq \frac{1}{2}x_{max}^*$ rather than the full support for our initialization. Therefore, our sample complexity depends on x_{max}^* , which is at least $1/\sqrt{k}$, rather than x_{min}^* , which can be at most $1/\sqrt{k}$. This is made precise in the following Lemma.

Lemma 1. (*Support recovery*) *Let $\mathbf{x}^* \in \mathbb{R}^n$ be any k -sparse vector with $x_{min}^* = \mathcal{O}(\frac{1}{\sqrt{k}})$, and let $\{Y_j = (\mathbf{A}_j^T \mathbf{x}^*)^2\}_{j=1}^m$ be m measurements, where $\mathbf{A}_j \sim \mathcal{N}(0, \mathbf{I}_n)$ are i.i.d. Gaussian vectors. If $m \geq \mathcal{O}(k(x_{max}^*)^{-2} \log n)$, then, with probability at least $1 - \mathcal{O}(n^{-10})$, choosing the largest instance in $\{\frac{1}{m} \sum_{j=1}^m Y_j A_{ji}^2\}$ returns an index i with $|x_i^*| \geq \frac{1}{2}x_{max}^*$. Further, let \mathbf{X}^1 be the estimate obtained from running one step of Algorithm 3 with any $\eta, \alpha \in (0, \frac{1}{10})$ (and $B = 1$, i.e. no multiple restarts). Then, with the same probability, we can recover the support $S = \{i : x_i^* \neq 0\}$ by choosing the k largest coordinates of $|\mathbf{X}^1|$ (where $|\cdot|$ denotes taking absolute values coordinate-wise).*

The proof of Lemma 1 relies on standard concentration results and is deferred to the appendix.

Lemma 1 shows that, provided knowledge of the sparsity level k , Algorithm 3 can be used to recover the support of a k -sparse signal \mathbf{x}^* from $\mathcal{O}(k(x_{max}^*)^{-2} \log n)$ Gaussian measurements, which, in the worst case, matches the best known bounds $\mathcal{O}(k^2 \log n)$ (Netrapalli et al., 2015; Wang et al., 2018), while it is an improvement if \mathbf{x}^* contains (at least) one large coordinate. For instance, if $x_{max}^* = \mathcal{O}(1)$, only $\mathcal{O}(k \log n)$ samples are required for support recovery.

We validate this theoretical result in the following experiment. Let $\mathbf{x}^* \in \mathbb{R}^{10000}$ be a k -sparse signal with randomly sampled support $S = \{i_1, \dots, i_k\} \subset [10000]$ and normalized to $\|\mathbf{x}^*\|_2 = 1$. We consider maximum signal values (i) $x_{max}^* = \frac{1}{\sqrt{k}}$, (ii) $x_{max}^* = k^{-0.25}$ and (iii) $x_{max}^* = 0.7$. In case (i), we set $x_{i_j}^* = \pm \frac{1}{\sqrt{k}}$ at random for all $j = 1, \dots, k$. For the cases (ii) and (iii), we fix $x_{i_1}^* = x_{max}^*$, sample the other components from $x_{i_j}^* \sim \mathcal{N}(0, 1)$ i.i.d., and then normalize them to satisfy $\|\mathbf{x}^*\|_2 = 1$. We also consider a signal with $x_{i_j}^* \sim \mathcal{N}(0, 1)$ i.i.d. normalized to $\|\mathbf{x}^*\|_2 = 1$, without any restrictions on x_{max}^* . We generate $m = 5000$ Gaussian measurements using (1) and $\mathbf{A}_j \sim \mathcal{N}(0, \mathbf{I}_n)$ i.i.d..

For our method (HWF) we run one step of Algorithm 3 and pick the k largest components of $|\mathbf{X}^1|$. We compare it with the support recovery methods used in SPARTA and SparseAltMinPhase (other algorithms like SWF and CRAF use the same support recovery method as SPARTA). Note that although correct identification of the full support is required for the theoretical guarantees of algorithms like SPARTA, it is not necessary in practice: it has been noted in (Wang et al., 2018) that, since the estimated support \hat{S} is only used for the orthogonality-promoting initialization, SPARTA is successful as long as the initial estimate is sufficiently close to the underlying signal (more precisely, $\text{dist}(\mathbf{X}^0, \mathbf{x}^*) \leq \frac{1}{10}\|\mathbf{x}^*\|_2$), regardless of whether or not the full support has been correctly identified. Intuitively, the initialization produces an estimate sufficiently close to \mathbf{x}^* as long as the majority of the support is recovered. This has been made rigorous for an alternative spectral initialization in (Jagtap and Hedge, 2017).

We evaluate the proportion of correctly recovered support variables

$$\frac{|\hat{S} \cap S|}{|\hat{S}|}$$

obtained from 100 independent Monte Carlo trials, where $\hat{S} \subset [n]$ denotes the estimated support.

Figure 1 confirms the predictions of Lemma 1. In the first case, where the signal only takes the values $x_i^* \in \{-\frac{1}{\sqrt{k}}, 0, \frac{1}{\sqrt{k}}\}$, our theoretical bound reads $\mathcal{O}(k^2 \log n)$, and we expect the support

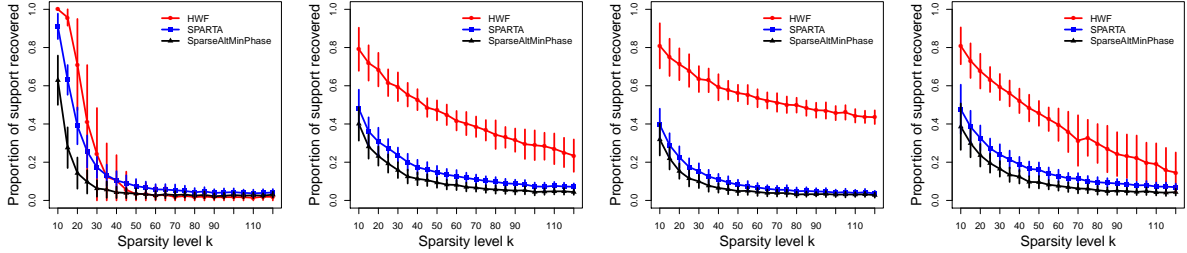


Figure 1: Proportion of support variables $|\hat{S} \cap S|/|S|$ correctly recovered plus/minus one standard deviation (vertical lines) by our method (red curve), SPARTA (blue curve) and SparseAltMinPhase (black curve), for different levels of x_{max}^* . From left to right: (i) $x_{max}^* = \frac{1}{\sqrt{k}}$, (ii) $x_{max}^* = k^{-0.25}$, (iii) $x_{max}^* = 0.7$, and (iv) Gaussian signal \mathbf{x}^* (without restrictions on x_{max}^*).

recovery performance of our method to be comparable to the other methods. For sparsity levels $k \geq 45$, our method is slightly worse than the other two, because it fails to identify a coordinate i with $x_i^* \neq 0$ in the first step. This case is of little practical relevance, since if only such a small portion of the support is recovered, neither of the three algorithms is able to reconstruct \mathbf{x}^* . As we increase x_{max}^* , the performance of our method improves substantially, while the support recovery methods used in SPARTA and SparseAltMinPhase do not show any improvement (in fact, they get slightly worse, which can be attributed to the fact that, as we increase x_{max}^* , the other coordinates become smaller since we keep $\|\mathbf{x}^*\|_2 = 1$ fixed). Our method also shows better support recovery performance in the case of a Gaussian signal \mathbf{x}^* , where we do not fix x_{max}^* (rightmost figure).

5 Parameter Estimation

In this section, we first demonstrate that our support recovery method, which coincides with one step of HWF, can be combined with existing algorithms (such as SPARTA) to give a final procedure which provably recovers a k -sparse signal from $\mathcal{O}(k(x_{max}^*)^{-2} \log n)$ measurements; this is summarized in Algorithm 4.

Algorithm 4: SPARTA with support, multiple restarts

Input: observations $\{Y_j\}_{j=1}^m$, measurement vectors $\{\mathbf{A}_j\}_{j=1}^m$, sparsity level k , step size η , iterations T , initialization size α , number of restarts B

Set i_1, \dots, i_B to the B largest instances in $\{\frac{1}{m} \sum_{j=1}^m Y_j A_{ji}^2\}$

for $b = 1$ **to** B **do**

Set $\mathbf{U}^0 = \mathbf{V}^0 = \alpha \mathbf{1}_n$, $U_{i_b}^0 = \left(\sqrt{\frac{1}{3}} + \alpha^2\right)^{\frac{1}{2}}$

Run one step of Algorithm 1 with $(\mathbf{U}^0, \mathbf{V}^0)$ for $\mathbf{X}^{1,b}$

Set \hat{S}_b to include the k largest coordinates of $|\mathbf{X}^{1,b}|$

Run T iterations of SPARTA using \hat{S}_b for $\mathbf{X}^{T,b}$

end for

Set b_{min} to be the index which minimizes $\|\nabla F(\mathbf{X}^{T,b})\|_2$

Return: $\mathbf{X}^{T,b_{min}}$

Note that we can allow multiple restarts in this case as well ($B > 1$) in order to further improve the probability of obtaining a good initialization. Since SPARTA only produces k -sparse solutions due to the thresholding step, we choose the final solution by selecting the one which produces the smallest gradient $\|\nabla F(\mathbf{X}^{T,b})\|_2$.

Our analysis from the previous section immediately leads to the following result.

Theorem 2. *Let $\mathbf{x}^* \in \mathbb{R}^n$ be any k -sparse vector with $x_{min}^* = \mathcal{O}(\frac{1}{\sqrt{k}})$, and let $\{Y_j = (\mathbf{A}_j^T \mathbf{x}^*)^2\}_{j=1}^m$ be m measurements, where $\mathbf{A}_j \sim \mathcal{N}(0, \mathbf{I}_n)$ are i.i.d. Gaussian vectors. If $m \geq \mathcal{O}(k(x_{max}^*)^{-2} \log n)$, then, with the parameters specified in (Wang et al., 2018), successive estimates of Algorithm 4 (a single run, i.e. $B = 1$) satisfy*

$$\text{dist}(\mathbf{X}^t, \mathbf{x}^*) \leq \frac{1}{10}(1 - \nu)^t \|\mathbf{x}^*\|_2, \quad t \geq 0,$$

with probability at least $1 - \mathcal{O}(m^{-1})$, where $0 < \nu < 1$ is a universal constant.

Proof. By Lemma 1, Algorithm 4 recovers the correct support with probability $1 - \mathcal{O}(n^{-10})$. With $\hat{S} = S$, the result follows from Lemma 2 and 3 of (Wang et al., 2018). \square

Compared to Theorem 1 of (Wang et al., 2018), this result reduces the sample complexity from $\mathcal{O}(k^2 \log n)$ to $\mathcal{O}(k(x_{max}^*)^{-2} \log n)$. The assumption $x_{min}^* = \mathcal{O}(1/\sqrt{k})$ is likely an artifact of the proof method of (Wang et al., 2018) and not necessary. Intuitively, identifying the full support is not necessary, as a good initialization can also be obtained if only small coordinates with $x_i^* \leq \mathcal{O}(1/\sqrt{m})$ are missed. This has been made rigorous for an alternative spectral initialization (Jagatap and Hedge, 2017). However, the orthogonality-promoting initialization used in SPARTA has been experimentally found to produce an initial estimate closer to the signal \mathbf{x}^* than the spectral initialization (Wang et al., 2017; Zhang et al., 2018).

One step of Algorithm 1 requires $\mathcal{O}(nm)$ operations and $T = \mathcal{O}(\log(1/\epsilon))$ SPARTA iterations are sufficient for $\text{dist}(\mathbf{X}^t, \mathbf{x}^*) \leq \epsilon$, so Algorithm 4 incurs a total computational cost of $\mathcal{O}(nm \log(1/\epsilon))$ to find an ϵ -accurate solution. This is, up to the logarithmic term $\log(1/\epsilon)$, proportional to the cost of reading the data.

However, Algorithm 4 comes with the disadvantage described in Section 1: sparsity of the estimates \mathbf{X}^t is enforced explicitly via a hard-thresholding step, which requires knowledge of the sparsity level k (or an upper bound). Our simulations show that HWF adapts to the signal sparsity k : we neither need knowledge of k for thresholding steps, nor do we need to add a penalty term to the objective function and tune regularization parameters in order to promote sparsity. Given enough samples, our algorithm automatically converges to the k -sparse signal \mathbf{x}^* .

In the following, we present simulations evaluating the reconstruction performance of Algorithms 3 and 4 relative to state-of-the-art methods for sparse phase retrieval. In particular, we will consider SPARTA, SWF and PR-GAMP.

Remark 1 (Comparison with PR-GAMP). *Our numerical experiments show favourable sample complexities for PR-GAMP compared to gradient based methods. PR-GAMP has been empirically shown to achieve linear sample complexity in some regimes with Gaussian signals (Schniter and Rangan, 2015). However, PR-GAMP relies on the implementation and tuning of several algorithmic principles, such as damping, normalization, and expectation-maximization (EM) steps. On the one hand, the application of these algorithmic principles makes PR-GAMP difficult to analyze, as rigorous theoretical investigations are known to be challenging even for much simpler AMP-based algorithms Bayati and Montanari (2011). On the other hand, running PR-GAMP requires tuning of several parameters, including the sparsity rate k/n via EM steps, and it requires choosing the prior distribution for the signal \mathbf{x}^* . The simulations we present are obtained using the freely available GAMP package¹ that does automatic parameter tuning,*

¹For PR-GAMP we used the code available from <https://sourceforge.net/projects/gampmatlab/>

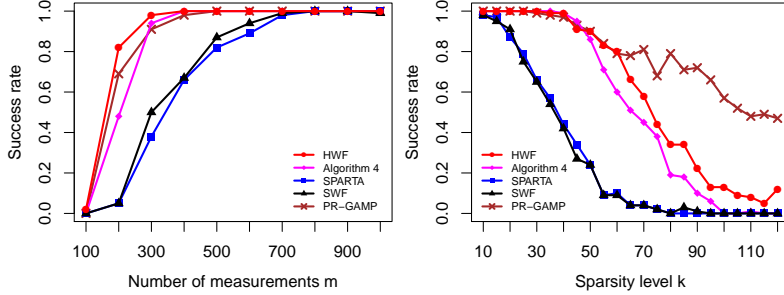


Figure 2: Empirical success rate for $n = 500$ fixed against number of measurements m with sparsity level $k = 20$ fixed (left) and against sparsity level k with $m = 500$ Gaussian measurements.

using the Gauss-Bernoulli prior. HWF is a much simpler algorithm, as it is just vanilla gradient descent applied to the unregularized empirical risk with Hadamard parametrization. HWF does not rely on algorithmic principles to promote convergence to good solutions, and it is empirically seen to adapt to the sparsity level k . We leave it to future work to give a full theoretical account on the convergence guarantees of HWF and to consider more refined and fine-tuned formulations of HWF that can combine algorithmic principles typically used in the literature on sparsity (cf. Section 6, Conclusion).

In experiments where we do not fix x_{max}^* , the true signal vector $\mathbf{x}^* \in \mathbb{R}^{500}$ was obtained by first sampling $\mathbf{x}^* \sim \mathcal{N}(0, \mathbf{I}_{500})$, then setting $(500 - k)$ random entries of \mathbf{x}^* to 0 and finally normalizing $\|\mathbf{x}^*\|_2 = 1$. Otherwise, \mathbf{x}^* is generated as described in Section 4. We obtain m observations via (1) with $\mathbf{A}_j \sim \mathcal{N}(0, \mathbf{I}_{500})$ i.i.d..

After trying a few choices of parameters for SPARTA and SWF, we found the values suggested in the original papers to work best in our simulations and used these in all experiments (also for the SPARTA part within Algorithm 4). For Algorithm 3 we found that, similar to WF without our parametrization, a constant step size of $\eta = 0.1$ works well (Ma et al., 2018). For the other parameters, any small values work well without much difference and we set $\alpha = 0.001$, $\kappa = 0.05$ and allow $B = 50$ restarts. We run all algorithms until $F(\mathbf{X}^t) \leq 10^{-7}$ or for a maximum of $T = 100000$ iterations, and declare it a success if the relative error

$$\frac{\text{dist}(\mathbf{X}^T, \mathbf{x}^*)}{\|\mathbf{x}^*\|_2}$$

is less than 0.01. We evaluate the empirical success rate obtained from 100 independent Monte Carlo trials.

In all experiments, SPARTA, SWF and Algorithm 4 were run with oracle knowledge of the true signal sparsity $\|\mathbf{x}^*\|_0 = k$. Knowledge of k is not required to run HWF. Note that in the absence of the knowledge of k , (Wang et al., 2018) uses an upper bound $\hat{k} = \sqrt{n}$ to run the algorithm, which is the theoretically affordable sparsity level. In our experiments we also consider larger sparsity levels $k > \sqrt{n}$, in which case this approach becomes futile.

In the first experiment we fix the sparsity level to $k = 20$ and vary m from 100 to 1000. Figure 2 (left plot) shows that HWF is able to reconstruct the signal reliably (with 95% success rate) from $m = 300$ Gaussian measurements, which is slightly better than PR-GAMP ($m = 400$), while SPARTA and SWF both require more than twice as many observations ($m = 700$). HWF also achieves slightly better reconstruction performance than Algorithm 4.

For the next experiment we fix $m = 500$ and vary the sparsity level k . Figure 2 (right plot) shows that both HWF and PR-GAMP achieve a reconstruction rate of 95% for signals with up

to 40 non-zero entries, while the SPARTA and SWF achieve this success rate only for signals with up to 15 non-zero entries. PR-GAMP is seen to achieve higher success rates than HWF for sparsity levels where neither algorithm is able to reliably reconstruct the signal.

In the previous section, we discussed the superior support recovery performance of our method as x_{max}^* increases. The next experiment examines whether this effect also translates into better reconstruction performance. To this end, we consider signals generated as in the experiments in Section 4, fix $m = 500$ and vary $k \in [10, 120]$. Figure 3 shows that, even when the signal only takes values $x_i^* \in \{-\frac{1}{\sqrt{k}}, 0, \frac{1}{\sqrt{k}}\}$, HWF achieves higher success rates than the SPARTA and SWF, while Algorithm 4 is comparable to them. This is expected, as also the support recovery performance is similar for this \mathbf{x}^* , and Algorithm 4 subsequently applies the same steps as SPARTA. As x_{max}^* increases, the reconstruction performance of our methods improves, with HWF maintaining a higher success rate than Algorithm 4. As before, the performance of PR-GAMP is comparable to HWF when considering the sparsity level up to which a 95% success rate is achieved, while PR-GAMP achieves higher success rates than HWF when neither algorithm reliably reconstructs the signal. PR-GAMP also shows improved success rates as x_{max}^* increases, which might explain the linear sample complexity observed in in some regimes (Schniter and Rangan, 2015) for Gaussian signals. The maximum component of a Gaussian vector scales (in expectation) like $\sqrt{\log k}/\sqrt{k}$, which is, if k is not very large, noticeably larger than $1/\sqrt{k}$. Comparing the right plot of Figure 2 and the left plot of Figure 3, we see that PR-GAMP achieves higher success rates for Gaussian signals than for the signal with $x_{max}^* = 1/\sqrt{k}$.

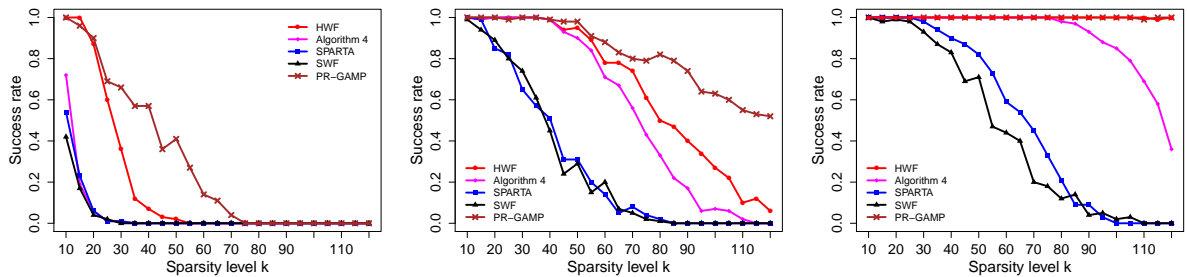


Figure 3: Empirical success rate against sparsity level k with $n = m = 500$ fixed. From left to right: (i) $x_{max}^* = 1/\sqrt{k}$, (ii) $x_{max}^* = k^{-0.25}$ and (iii) $x_{max}^* = 0.7$.

Next, we examine how the sample complexity of HWF scales with the signal sparsity k . The success rate vs signal sparsity k and number of measurements m is shown in Figure 4, which suggests that the sample complexity scales as $\mathcal{O}(k(x_{max}^*)^{-2} \log \frac{n}{k})$, where we obtain x_{max}^* as the average maximum coordinate of 100000 Gaussian k -sparse signals. We note that this scaling seems to be almost linear.

One of the parameters in Algorithm 3 is the number of restarts B . Increasing B also increases the probability of HWF finding the true signal, but this comes at the cost of an increase in computational time. For the next experiment we run HWF in the same setting as the first two experiments and vary the number of allowed restarts B from 1 to 100. Figure 5 shows that increasing the number of allowed restarts indeed increases the probability of successful reconstruction, where the success rate barely increases further as we increase the number of restarts B beyond 50.

Finally, we examine the convergence behavior of HWF. We also test HWF in the complex-valued setting, where we generate vectors \mathbf{x}^* , $\mathbf{A}_j \sim \mathcal{N}(0, \frac{1}{2}\mathbf{I}_{500}) + i\mathcal{N}(0, \frac{1}{2}\mathbf{I}_{500})$, set 490 random entries of \mathbf{x}^* to zero, normalize $\|\mathbf{x}^*\|_2 = 1$ and generate m measurements according to (1). Figure 6

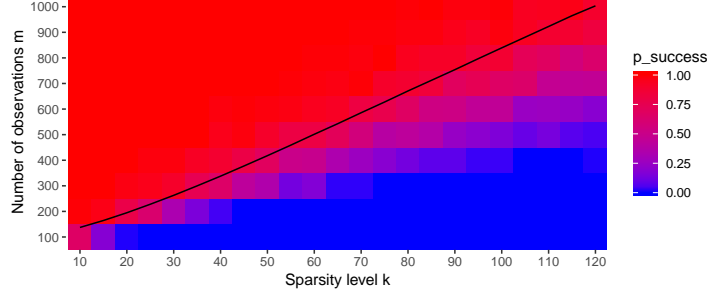


Figure 4: Empirical success rate (red: high, blue: low) of HWF against sparsity level k and number of observations m , with $n = 500$ fixed. Black line: $m = \frac{1}{3}k(x_{max}^*)^{-2} \log \frac{n}{k}$.

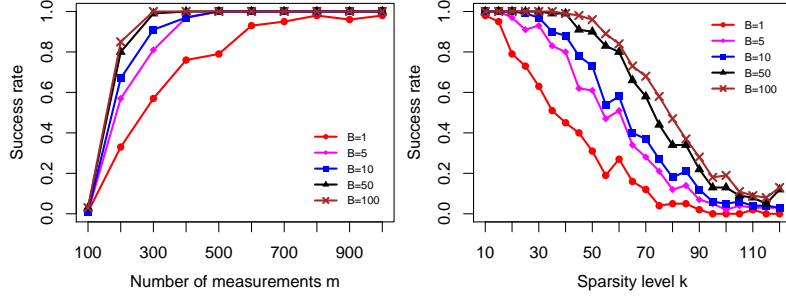


Figure 5: Empirical success rate against number of measurements m (left) and sparsity level k (right) with $n = 500$ fixed, for different numbers of restarts $B \in [1, 100]$.

shows that HWF is also able to reconstruct complex signals. While HWF converges faster in the real case, both cases exhibit sublinear convergence after a short “warm-up” period. This can be explained by our parametrization. Consider the gradient $\nabla_{\mathbf{u}} F(\mathbf{U}^t, \mathbf{V}^t) = 2\nabla F(\mathbf{X}^t) \odot \mathbf{U}^t$: as the initialization size α is small, the gradient is small in the beginning due to the term \mathbf{U}^t . As \mathbf{X}^t approaches \mathbf{x}^* , the term $\nabla F(\mathbf{X}^t)$ converges to zero, which leads to linear convergence with a constant stepsize in the case of WF (Ma et al., 2018). With our parametrization, $\nabla_{\mathbf{u}} F$ (or $\nabla_{\mathbf{v}} F$) converges to zero faster than $\nabla_{\mathbf{x}} F$, as we typically have $U_i^t \rightarrow 0$ or $V_i^t \rightarrow 0$ (or both, if $x_i^* = 0$), leading to sublinear convergence.

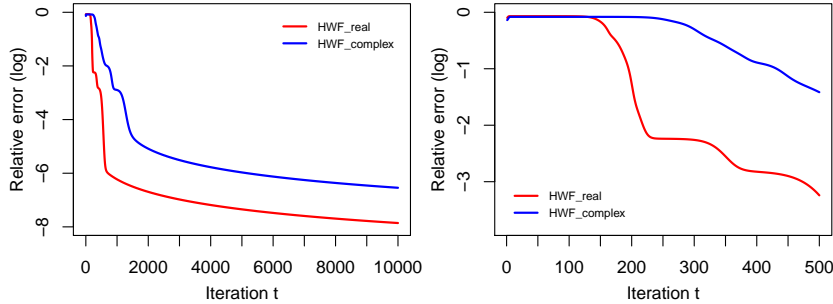


Figure 6: Relative error (log-scale) of HWF for real/complex signals for 10000 iterations (left) and zoom-in to 500 iterations (right).

6 Conclusion

In this paper we proposed HWF, which is a simple algorithm for sparse phase retrieval. We proved that one step of HWF can be used as a support recovery tool, which, combined with existing algorithms such as SPARTA, yields a computationally fast algorithm with improved sample complexity, which reads $\mathcal{O}(k \log n)$ if the signal contains at least one large component. We have shown in numerical experiments that the sample complexity of HWF is lower than that of other gradient based methods such as SPARTA and SWF, and comparable to PR-GAMP, which has been empirically shown to achieve linear sample complexity for Gaussian signals (Schniter and Rangan, 2015). While HWF does not require knowledge of the signal sparsity k or any added regularization terms, this simplicity seems to come at the price of sublinear convergence and thus increased computational cost. We leave it to future work to investigate whether algorithmic principles such as the increasing step-size scheme considered in (Vaškevičius et al., 2019) or thresholding steps previously considered in the literature on sparse phase retrieval (e.g. (Cai et al., 2016; Wang et al., 2018; Zhang et al., 2018)) can be used to accelerate the convergence speed of HWF or to further improve its sample complexity to the level of the empirical results seen for PR-GAMP, which already relies on combinations of many such algorithmic principles (damping, normalization, EM steps). Compared to PR-GAMP, the simplicity of HWF makes the algorithm more amenable to a rigorous theoretical investigation that can support the high-level analysis presented in our work.

References

- S. Arora, N. Cohen, W. Hu, and Y. Luo. Implicit regularization in deep matrix factorization. In *Advances in Neural Information Processing Systems*, pages 7411–7422, 2019.
- R. Balan, P. Casazza, and D. Edidin. On signal reconstruction without phase. *Computational Harmonic Analysis*, 20(3):345–356, 2006.
- M. Bayati and A. Montanari. The dynamics of message passing on dense graphs, with applications to compressed sensing. *IEEE Transactions on Information Theory*, 57(2):764–785, 2011.
- O. Bunk, A. Diaz, F. Pfeiffer, C. David, B. Schmitt, D. K. Satapathy, and J. F. Veen. Diffractive imaging for periodic samples: Retrieving one-dimensional concentration profiles across microfluidic channels. *Acta Crystallographica Section A: Foundations of Crystallography*, 63(4):306–314, 2007.
- T. Cai, X. Li, and Z. Ma. Optimal rates of convergence for noisy sparse phase retrieval via thresholded Wirtinger flow. *Annals of Statistics*, 44(5):2221–2251, 2016.
- E. J. Candès and X. Li. Solving quadratic equations via PhaseLift when there are about as many equations as unknowns. *Foundations of Computational Mathematics*, 14(5):1017–1026, 2012.
- E. J. Candès, T. Strohmer, and V. Voroninski. PhaseLift: Exact and stable signal recovery from magnitude measurements via convex programming. *Communications on Pure and Applied Mathematics*, 66(8):1241–1274, 2013.
- E. J. Candès, X. Li, and M. Soltanolkotabi. Phase retrieval via Wirtinger flow: Theory and algorithms. *IEEE Transactions on Information Theory*, 61(4):1985–2007, 2015.

- Y. Chen and E. J. Candès. Solving random quadratic systems of equations is nearly as easy as solving linear systems. In *Advances in Neural Information Processing Systems*, pages 739–747, 2015.
- Y. Chen, Y. Chi, J. Fan, and C. Ma. Gradient descent with random initialization: Fast global convergence for nonconvex phase retrieval. *Mathematical Programming*, 176(1–2):5–37, 2019.
- F. Chung and L. Lu. Concentration inequalities and martingale inequalities: a survey. *Internet Math.*, 3(1):79–127, 2006.
- Y. C. Eldar and S. Mendelson. Phase retrieval: Stability and recovery guarantees. *Applied and Computational Harmonic Analysis*, 36(3):473–494, 2014.
- J. R. Fienup. Phase retrieval algorithms: A comparison. *Applied Optics*, 21(15):2758–2769, 1982.
- R. W. Gerchberg and W. O. Saxton. A practical algorithm for the determination of phase from image and diffraction. *Optik*, 35:237–246, 1972.
- T. Goldstein and C. Studer. PhaseMax: Convex phase retrieval via basis pursuit. *IEEE Transactions on Information Theory*, 64(4):2675–2689, 2018.
- S. Gunasekar, B. E. Woodworth, S. Bhojanapalli, B. Neyshabur, and N. Srebro. Implicit regularization in matrix factorization. In *Advances in Neural Information Processing Systems*, pages 6151–6159, 2017.
- P. Hand and V. Voroninski. Compressed sensing from phaseless Gaussian measurements via linear programming in the natural parameter spaces. *arXiv preprint arXiv:1611.05985*, 2016.
- P. D. Hoff. Lasso, fractional norm and structured sparse estimation using a Hadamard product parametrization. *Computational Statistics & Data Analysis*, 115:186–198, 2017.
- K. Jaganathan, S. Oymak, and B. Hassibi. Sparse phase retrieval: Convex algorithms and limitations. In *Proceedings of IEEE International Symposium on Information Theory*, pages 1022–1026, 2013.
- K. Jaganathan, Y. C. Eldar, and B. Hassibi. Phase retrieval: An overview of recent developments. In A. Stern, editor, *Optical Compressive Imaging*, chapter 13, pages 263–296. Taylor Francis Group, Boca Raton, FL, 2016.
- G. Jagatap and C. Hedge. Fast, sample-efficient algorithms for structured phase retrieval. In *Advances in Neural Information Processing Systems*, pages 4917–4927, 2017.
- G. Jagatap and C. Hedge. Sample-efficient algorithms for recovering structured signals from magnitude-only measurements. *IEEE Transactions on Information Theory*, 65(7):4434–4456, 2019.
- X. Li and V. Voroninski. Sparse signal recovery from quadratic measurements via convex programming. *SIAM Journal on Mathematical Analysis*, 45(5):3019–3033, 2013.
- Y. Li, T. Ma, and H. Zhang. Algorithmic regularization in over-parametrized matrix sensing and neural networks with quadratic activation. In *Conference on Learning Theory*, pages 2–47, 2018.
- C. Ma, K. Wang, Y. Chi, and Y. Chen. Implicit regularization in nonconvex statistical estimation: Gradient descent converges linearly for phase retrieval and matrix completion. In *International Conference on Machine Learning*, pages 3345–3354, 2018.

- R. Millane. Phase retrieval in crystallography and optics. *JOSA A*, pages 394–411, 1990.
- P. Netrapalli, P. Jain, and S. Sanghavi. Phase retrieval using alternating minimization. *IEEE Transactions on Signal Processing*, 63(18):4814–4826, 2015.
- H. Ohlsson, A. Y. Yang, R. Dong, and S. S. Sastry. CPRL—an extension of compressive sensing to the phase retrieval problem. In *Advances in Neural Information Processing Systems*, pages 1367–1375, 2012.
- T. Qiu and D. P. Palomar. Undersampled sparse phase retrieval via majorization–minimization. *IEEE Transactions on Signal Processing*, 65(22):5957–5969, 2017.
- Y. Schechtman, A. Beck, and Y. C. Eldar. GESPAR: Efficient phase retrieval of sparse signals. *IEEE Transactions on Signal Processing*, 62(4):928–938, 2014.
- P. Schniter and S. Rangan. Compressive phase retrieval via generalized approximate message passing. *IEEE Transactions on Signal Processing*, 63(4):1043–1055, 2015.
- J. Sun, Q. Qu, and J. Wright. A geometric analysis of phase retrieval. *Foundations of Computational Mathematics*, 18(5):1131–1198, 2018.
- T. Vaškevičius, V. Kanade, and P. Rebeschini. Implicit regularization for optimal sparse recovery. In *Advances in Neural Information Processing Systems*, pages 2968–2979, 2019.
- V. Voroninski and Z. Xu. A strong restricted isometry property, with an application to phaseless compressed sensing. *Applied and Computational Harmonic Analysis*, 40(2):386–395, 2016.
- I. Waldspurger, A. d’Aspremont, and S. Mallat. Phase recovery, MaxCut and complex semidefinite programming. *Mathematical Programming*, 149(1-2):47–81, 2015.
- G. Wang, G. B. Giannakis, and Y. C. Eldar. Solving systems of random quadratic equations via truncated amplitude flow. *IEEE Transactions on Information Theory*, 64(2):773–794, 2017.
- G. Wang, L. Zhang, G. B. Giannakis, M. Akçakaya, and J. Chen. Sparse phase retrieval via truncated amplitude flow. *IEEE Transactions on Signal Processing*, 66(2):479–491, 2018.
- Z. Yang, C. Zhang, and L. Xie. Robust compressive phase retrieval via L1 minimization with application to image reconstruction. *arXiv preprint arXiv:1302.0081*, 2013.
- Z. Yuan, H. Wang, and Q. Wang. Phase retrieval via sparse Wirtinger flow. *Journal of Computational and Applied Mathematics*, 355:162–173, 2019.
- H. Zhang, Y. Zhou, Y. Liang, and Y. Chi. A nonconvex approach for phase retrieval: Reshaped Wirtinger flow and incremental algorithms. *Journal of Machine Learning Research*, 18(141):1–35, 2017.
- L. Zhang, G. Wang, G. B. Giannakis, and J. Chen. Compressive phase retrieval via reweighted amplitude flow. *IEEE Transactions on Signal Processing*, 66(19):5029–5040, 2018.
- P. Zhao, Y. Yang, and Q.-C. He. Implicit regularization via Hadamard product over-parametrization in high-dimensional linear regression. *arXiv preprint arXiv:1903.09367*, 2019.

A Proof of Lemma 1

In the following, we assume, without loss of generality, that $\|\mathbf{x}^*\|_2 = 1$; this assumption is made purely for notational simplicity, since we then have $x_{max}^* = \max_i \frac{|x_i^*|}{\|\mathbf{x}^*\|_2} = \max_i |x_i^*|$ and $x_{min}^* = \min_{i:x_i^* \neq 0} \frac{|x_i^*|}{\|\mathbf{x}^*\|_2} = \min_{i:x_i^* \neq 0} |x_i^*|$. If $\|\mathbf{x}^*\|_2 \neq 1$ is unknown, then we only need to replace x_{max}^* and x_{min}^* with $\max_i |x_i^*| = x_{max}^* \|\mathbf{x}^*\|_2$ and $\min_{i:x_i^* \neq 0} |x_i^*| = x_{min}^* \|\mathbf{x}^*\|_2$ respectively in the following proof. Further, note that knowledge of $\|\mathbf{x}^*\|_2$ is not required for HWF.

The proof of Lemma 1 relies on the following result, which is a combination of Theorems 3.6 and 3.7 of (Chung and Lu, 2006).

Theorem 3. (Chung and Lu, 2006) *Let X_i be independent random variables satisfying $|X_i| \leq M$ for all $i \in [n]$. Let $X = \sum_{i=1}^n X_i$ and $\|X\| = \sqrt{\sum_{i=1}^n \mathbb{E}[X_i^2]}$. Then, we have*

$$\mathbb{P}[|X - \mathbb{E}[X]| > \lambda] \leq 2 \exp\left(-\frac{\lambda^2}{2(\|X\|^2 + M\lambda/3)}\right).$$

Proof of the first claim.

We first show that by choosing the largest instance in $\{\frac{1}{m} \sum_{j=1}^m Y_j A_{ji}^2\}$, we obtain an index i with $|x_i^*| \geq \frac{x_{max}^*}{2}$ with high probability. Recall that we write $R_i = \frac{1}{m} \sum_{j=1}^m Y_j A_{ji}^2$. We can compute

$$\begin{aligned} \mathbb{E}[R_i] &= \mathbb{E}[(\mathbf{A}_1^T \mathbf{x}^*)^2 A_{1i}^2] \\ &= \mathbb{E}[A_{1i}^4 (x_i^*)^2 + (\mathbf{A}_{1,-i}^T \mathbf{x}_{-i}^*)^2 A_{1i}^2] \\ &= 3(x_i^*)^2 + \|\mathbf{x}_{-i}^*\|_2^2 \\ &= \|\mathbf{x}^*\|_2^2 + 2(x_i^*)^2, \end{aligned}$$

where we denote by $\mathbf{x}_{-i} \in \mathbb{R}^{n-1}$ the vector obtained by deleting the i -th entry from $\mathbf{x} \in \mathbb{R}^n$ and use the fact that $A_{ji} \sim \mathcal{N}(0, 1)$ i.i.d. and hence $\mathbf{A}_{j,-i}^T \mathbf{x}_{-i} \sim \mathcal{N}(0, \|\mathbf{x}_{-i}^*\|_2^2)$, as $\mathbf{x}^* \in \mathbb{R}^n$ is a fixed vector independent of $\{A_{ji}\}$.

Let $i_{max} = \operatorname{argmax}_i R_i$. By definition, $R_{i_{max}} \geq R_i$ holds for all $i \in [n]$. If we can show $|R_i - \mathbb{E}[R_i]| \leq \frac{3}{4}(x_{max}^*)^2$ for all $i \in [n]$, then this would imply

$$\begin{aligned} \|\mathbf{x}^*\|_2^2 + 2(x_{i_{max}}^*)^2 &= \mathbb{E}[R_{i_{max}}] \\ &= \mathbb{E}[R_i] + (R_i - \mathbb{E}[R_i]) + (\mathbb{E}[R_{i_{max}}] - R_{i_{max}}) + (R_{i_{max}} - R_i) \\ &\geq \mathbb{E}[R_i] - 2 \max_j |R_j - \mathbb{E}[R_j]| \\ &\geq \|\mathbf{x}^*\|_2^2 + 2(x_i^*)^2 - \frac{3}{2}(x_{max}^*)^2, \end{aligned}$$

for any $i \in [n]$. In particular, if we choose $i = \operatorname{argmax}_j |x_j^*|$, this implies $|x_{i_{max}}^*| \geq \frac{1}{2}x_{max}^*$, which concludes the proof of the first claim.

In order to show $|R_i - \mathbb{E}[R_i]| \leq \frac{3}{4}(x_{max}^*)^2$, we use the following truncation trick: write

$$R_i = \frac{1}{m} \sum_{j=1}^m Y_j A_{ji}^2 = \frac{1}{m} \sum_{j=1}^m (\mathbf{A}_j^T \mathbf{x}^*)^2 A_{ji}^2 = \frac{1}{m} \sum_{j=1}^m (Z_{1,j} + Z_{2,j}),$$

where $Z_{1,j} = (\mathbf{A}_j^T \mathbf{x}^*)^2 A_{ji}^2 \cdot \mathbf{1}(\max\{|\mathbf{A}_j^T \mathbf{x}^*|, |A_{ji}|\} < \sqrt{44 \log n})$ and $Z_{2,j} = (\mathbf{A}_j^T \mathbf{x}^*)^2 A_{ji}^2 - Z_{1,j}$. Since $Z_{1,j}$ is bounded, we can apply Theorem 3. To this end, compute the second moment

$$\sqrt{\sum_{j=1}^m \frac{1}{m^2} \mathbb{E}[Z_{1,j}]} \leq \sqrt{\sum_{j=1}^m \frac{1}{m^2} \mathbb{E}[(\mathbf{A}_j^T \mathbf{x}^*)^2 A_{ji}^2]} \leq \sqrt{\sum_{j=1}^m \frac{1}{m^2} \left(\mathbb{E}[(\mathbf{A}_j^T \mathbf{x}^*)^4] \mathbb{E}[A_{ji}^4] \right)^{\frac{1}{2}}} \leq \sqrt{\frac{3}{m}},$$

where we used the Cauchy-Schwarz inequality and the fact that $\mathbf{A}_j^T \mathbf{x}^* \sim \mathcal{N}(0, 1)$. With this, we have

$$\mathbb{P} \left[\left| \frac{1}{m} \sum_{j=1}^m Z_{1,j} - \mathbb{E}[Z_{1,j}] \right| > \frac{3}{8} (x_{max}^*)^2 \right] \leq 2 \exp \left(\frac{\frac{9}{64} (x_{max}^*)^4}{2 \left(\frac{3}{m} + 44^2 \log^2 n \cdot \frac{3}{4} (x_{max}^*)^2 / 3 \right)} \right) \leq \mathcal{O}(n^{-11})$$

since $m \geq \mathcal{O}(k(x_{max}^*)^{-2} \log n)$.

For the second term $Z_{2,j}$, we can use the Chebyshev inequality: we have

$$\begin{aligned} \text{Var} \left(\frac{1}{m} \sum_{j=1}^m Z_{2,j} \right) &\leq \frac{1}{m} \mathbb{E} \left[(\mathbf{A}_j^T \mathbf{x}^*)^2 A_{ji}^2 \cdot \mathbf{1} \left(\max\{|\mathbf{A}_j^T \mathbf{x}^*|, |A_{ji}|\} > \sqrt{44 \log n} \right) \right] \\ &\leq \frac{1}{m} \sqrt{\mathbb{E}[(\mathbf{A}_j^T \mathbf{x}^*)^4 A_{ji}^4]} \cdot \mathbb{P} \left[\max\{|\mathbf{A}_j^T \mathbf{x}^*|, |A_{ji}|\} > \sqrt{44 \log n} \right] \\ &\leq \frac{\sqrt{105}}{m} \cdot 2n^{-11}, \end{aligned}$$

and hence, by the Chebyshev inequality,

$$\mathbb{P} \left[\left| \frac{1}{m} \sum_{j=1}^m Z_{2,j} - \mathbb{E}[Z_{2,j}] \right| > \frac{3}{8} (x_{max}^*)^2 \right] \leq \frac{\frac{\sqrt{105}}{m} \cdot 2n^{-11}}{\frac{9}{64} (x_{max}^*)^4} \leq \mathcal{O}(n^{-11}).$$

Put together, this implies that

$$\mathbb{P} \left[|R_i - \mathbb{E}[R_i]| > \frac{3}{4} (x_{max}^*)^2 \right] \leq \mathcal{O}(n^{-11}).$$

Taking the union bound over all $i \in [n]$ implies that $|R_i - \mathbb{E}[R_i]| \leq \frac{3}{4} (x_{max}^*)^2$ holds for all $i \in [n]$ with probability at least $1 - \mathcal{O}(n^{-10})$. This concludes the proof of the first claim of Lemma 1.

Proof of the second claim.

First, note that the gradient of the empirical risk $F(\mathbf{x})$ is given by

$$\nabla F(\mathbf{x}) = \frac{1}{m} \sum_{j=1}^m \left((\mathbf{A}_j^T \mathbf{x})^2 - (\mathbf{A}_j^T \mathbf{x}^*)^2 \right) (\mathbf{A}_j^T \mathbf{x}) \mathbf{A}_j.$$

By dominated convergence, the gradient of the population risk $f(\mathbf{x})$ can then be computed as

$$\begin{aligned} \nabla f(\mathbf{x}) &= \mathbb{E}[\nabla F(\mathbf{x})] = \mathbb{E} \left[\left((\mathbf{A}_1^T \mathbf{x})^2 - (\mathbf{A}_1^T \mathbf{x}^*)^2 \right) (\mathbf{A}_1^T \mathbf{x}) \mathbf{A}_1 \right] \\ &= (3\|\mathbf{x}\|_2^2 - 1)\mathbf{x} - 2(\mathbf{x}^T \mathbf{x}^*)\mathbf{x}^* \end{aligned}$$

for any fixed vector $\mathbf{x} \in \mathbb{R}^n$. Further, we have the initialization

$$U_i^0 = \begin{cases} \left(\sqrt{\frac{1}{3}} - \alpha^2 \right)^{\frac{1}{2}} & i = i_{max} \\ \alpha & i \neq i_{max} \end{cases}$$

$$V_i^0 = \alpha$$

which leads to

$$X_i^0 = \begin{cases} \sqrt{\frac{1}{3}} & i = i_{max} \\ 0 & i \neq i_{max} \end{cases}$$

Hence, we have

$$\nabla f(\mathbf{X}^0)_i = -\frac{2}{\sqrt{3}}x_{i_{max}}^*x_i^*.$$

In particular, $\nabla f(\mathbf{X}^0)_j = 0$ for $j \notin S$. Assume without loss of generality $x_{i_{max}}^* > 0$.

For the second claim we need to show that $|X_i^1| > |X_j^1|$ holds whenever $i \in S$ and $j \notin S$. First, consider the case $i \neq i_{max}$. Since $|X_i^1| = |(U_i^1)^2 - (V_i^1)^2|$, it suffices to show, assuming $x_i^* > 0$, that

$$U_i^1 > \max\{U_j^1, V_j^1\} \quad (5)$$

$$V_i^1 < \min\{U_j^1, V_j^1\} \quad (6)$$

holds simultaneously. The case $x_i^* < 0$ can be dealt with the same way, exchanging the roles of U_i^1 and V_i^1 . We have

$$\begin{aligned} U_i^1 &= \alpha \cdot (1 - 2\eta \nabla F(\mathbf{X}^0)_i) \\ &\geq \alpha \cdot \left(1 - 2\eta \nabla f(\mathbf{X}^0)_i - 2\eta \left| \nabla F(\mathbf{X}^0)_i - \nabla f(\mathbf{X}^0)_i \right| \right), \end{aligned}$$

and

$$U_j^1 \leq \alpha \cdot \left(1 + 2\eta \left| \nabla F(\mathbf{X}^0)_j - \nabla f(\mathbf{X}^0)_j \right| \right).$$

Now, $-\nabla f(\mathbf{X}^0)_i = \frac{2}{\sqrt{3}}x_{i_{max}}^*x_i^* \geq \frac{1}{\sqrt{3}}x_{max}^*x_{min}^*$, since from the first part we know that $x_{i_{max}}^* \geq \frac{1}{2}x_{max}^*$ and we assumed $x_i^* > 0$. Hence, if we can show

$$\max_i \left| \nabla F(\mathbf{X}^0)_i - \nabla f(\mathbf{X}^0)_i \right| \leq \frac{1}{2\sqrt{3}}x_{max}^*x_{min}^*, \quad (7)$$

then $U_i^1 \geq U_j^1$ follows. We also have

$$V_j^1 \leq \alpha \cdot \left(1 + 2\eta \left| \nabla F(\mathbf{X}^0)_j - \nabla f(\mathbf{X}^0)_j \right| \right),$$

which then implies $U_i^1 \geq V_j^1$, completing the proof of (5); (6) can be shown the same way.

The case $i = i_{max}$ also follows from (7). We can bound

$$\begin{aligned} \left| \nabla F(\mathbf{X}^0)_i \right| &\leq \left| \nabla f(\mathbf{X}^0)_i \right| + \left| \nabla F(\mathbf{X}^0)_i - \nabla f(\mathbf{X}^0)_i \right| \\ &\leq \frac{2}{\sqrt{3}}(x_{max}^*)^2 + \frac{1}{2\sqrt{3}}x_{max}^*x_{min}^* \\ &\leq \frac{2}{\sqrt{3}} + \frac{1}{2\sqrt{3}} \\ &\leq 2 \end{aligned}$$

Since we assume $\eta \leq 0.1$, we can bound

$$|2\eta \nabla F(\mathbf{X}^0)_i| \leq 0.4,$$

which, since also $\alpha \leq 0.1$, implies

$$U_i^1 \geq 3 \max\{U_j^1, V_j^1, V_i^1\},$$

and hence

$$|X_i^1| = (U_i^1)^2 - (V_i^1)^2 \geq 8 \max \left\{ (U_j^1)^2, (V_j^1)^2 \right\} \geq |X_j^1|.$$

What is left to show is (7). Since \mathbf{X}^0 is not independent from $\{A_{ji}\}$, define the (deterministic) vectors $\mathbf{x}^{(l)} \in \mathbb{R}^n$ for $l = 1, \dots, n$ by

$$x_i^{(l)} = \begin{cases} \sqrt{\frac{1}{3}} & i = l \\ 0 & i \neq l \end{cases}$$

Now, we need to show that the empirical gradient

$$\nabla F(\mathbf{x}^{(l)})_i = \frac{1}{m} \sum_{j=1}^m ((\mathbf{A}_j^T \mathbf{x}^{(l)})^2 - (\mathbf{A}_j^T \mathbf{x}^*)^2) (\mathbf{A}_j^T \mathbf{x}^{(l)}) A_{ji}$$

is close to its expectation $\nabla f(\mathbf{x}^{(l)})_i$. Using the same truncation trick as in the proof of the first claim, we can show

$$\mathbb{P} \left[\left| \nabla f(\mathbf{x}^{(l)})_i - \nabla F(\mathbf{x}^{(l)})_i \right| \geq \frac{1}{2\sqrt{3}} x_{max}^* x_{min}^* \right] \leq \mathcal{O}(n^{-12}),$$

Taking the union bound over all i and l implies that

$$\max_l \max_i |\nabla F(\mathbf{x}^{(l)})_i - \nabla f(\mathbf{x}^{(l)})_i| \leq \frac{1}{2\sqrt{3}} x_{max}^* x_{min}^*$$

holds with probability $1 - \mathcal{O}(n^{-10})$. Since $\mathbf{X}^0 = \mathbf{x}^{(i_{max})}$, this completes the proof of (7) and therefore of Lemma 1. \square